Distributed coordination strategy for target-enclosing operations by particle swarms

TAE-HYOUNG KIM
Chung-Ang University
School of Mechanical Engineering
221 Heukseok-dong, Dongjak-gu, Seoul
REPUBLIC OF KOREA
kimth@cau.ac.kr

Abstract: This paper presents a methodology for group coordination and cooperative control of n agents to achieve a target-enclosing operation in three-dimensional (3D) space. In the developed coordination strategy, multiple agents are controlled in a distributed manner to converge to an assigned formation while tracking the target object moving in 3D space. The distinctive features of the proposed method are as follows: First, it is a simple, memory-less control scheme. Second, no communication mechanism between agents is necessary, and thus it is inherently a distributed control strategy. From these viewpoints, it seems easy to implement. Further, it appears to be a practical method for the following reasons: (i) it is robust against any finite number of transient measurement errors and (ii) it can achieve the control objectives even when constraints on the control input exist. We also present a scheme to decrease the possibility of a collision between agents. Numerical examples are given to illustrate the efficacy of the proposed method and the achievement of an assigned formation in 3D space.

Key-Words: Multi-agent systems, distributed coordination, cooperative robot systems, circulant matrices

1 Introduction

Formation control, which coordinates the motions of relatively simple and inexpensive multiple agents, is one of the essential technologies that enable agents to cover a larger operational area and achieve complex tasks. Recently, several research groups developed coordination control strategies capable of achieving an enclosing formation around a specific area (object) by multiple agents using local information (see e.g. [1, 2, 3, 4, 5, 6, 7]). This type of coordination of motion is not only interesting but also significant because it has many potential applications from an engineering standpoint, as mentioned in Marshall et al. [2, 3] and Sepulchre et al. [5]. For instance, it is useful when hazardous terrestrial/oceanographic exploration, military surveillance, and rescue operations are performed by cooperative multi-agent systems.

In this line of research, Marshall et al. [2, 3] proposed a formation control method under cyclic pursuit for multiple agents with motion constraints moving in a plane. Based on the above methodology, Kim and Sugie [6, 7] proposed a distributed cooperative control scheme using a cyclic pursuit strategy for target-capturing tasks in three-dimensional (3D) space by multi-agent systems. In the above method, each agent's behavior is determined by using local information on the target object and*one* other agent in its neighborhood. For target-capturing strategies, Kobayashi et al. [4] suggested a decentralized control law based on a gradient descent method for multiple agents. However, in their method, each agent requires information on the target object and*two* other agents.

The above methods [2, 3, 4, 6, 7] guarantee that agents' coordination finally results in a circular formation. However, we cannot directly place each agent at the required location by these methods. Further, if the control schemes of Marshall et al. [2, 3] and Kim and Sugie [6, 7] are applied, each agent circulates continuously while maintaining a constant distance to its pursuing agent. Thus, the applicability of the given methods may be limited. Therefore, it is required within the framework of practical applicability to extend these approaches so that multiple agents are controlled in a distributed manner such that they converge to an assigned formation while tracking a target object moving in 3D space.

This paper proposes a distributed coordination strategy by which multiple agents converge to the formation assigned by the designer while tracking a target object moving in 3D space. To that purpose, we first consider a group of n agents randomly dispersed in 3D space. Then, based on the modification of the results by Kim and Sugie [6, 7], simple distributed

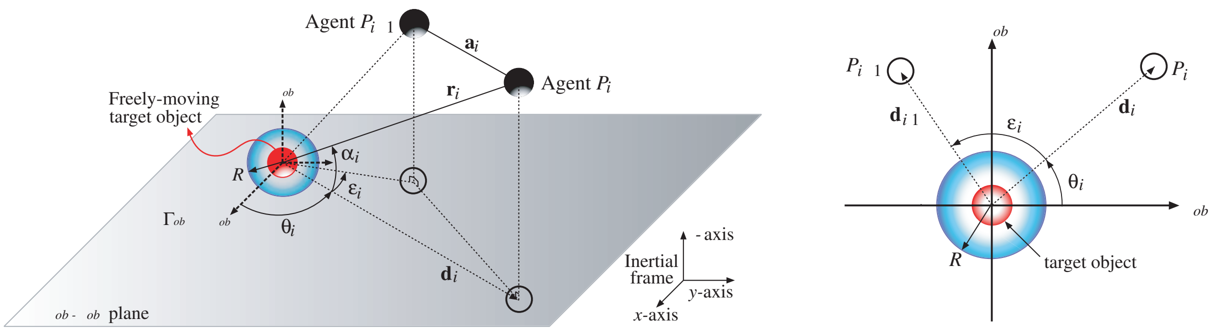

Figure 1: Coordinate frames and notations.

control laws are developed. This coordination strategy guarantees the achievement of the desired global behaviors of the agents by using only locally available information; each agent individually decides its behavior based on local information on only one other agent and the target object, which is probably minimum. This scheme can thus reduce the information requirements as compared with conventional methods. In the numerical examples, we verify that (i) the proposed method is robust against any finite number of transient measurement errors and (ii) it can achieve the control objectives even when constraints on the control input exist. From the above viewpoint, the proposed method is practical and easily implemented. A scheme to decrease the possibility of a collision between agents is also proposed, and its effectiveness is verified through a simulation study. Note that the agent dynamics are not considered and full actuation is assumed in this paper.

2 Problem Statement

Consider a group of n agents dispersed in 3D space, as shown in Figure 1. Each agent is modeled as an autonomous point mass and all agents are ordered from 1 to n; *i.e.*, $P_1, P_2, \cdots, P_n$. The position vectors of the target object and agent P_i $(i = 1, 2, \cdots, n)$ in the inertial frame are denoted by $\mathbf{p}_o(t) \in \mathbb{R}^3$ and $\mathbf{p}_i(t) \in \mathbb{R}^3$, respectively. Suppose that each agent is described as

$$\dot{\mathbf{p}}_i = \mathbf{u}_i, \tag{1}$$

where $\mathbf{u}_i \in \mathbb{R}^3$ is the control input. It is assumed that agent P_i can measure the following vectors:

$$\mathbf{r}_i \ (:= \mathbf{p}_i - \mathbf{p}_o), \ \ \mathbf{a}_i \ (:= \mathbf{p}_i - \mathbf{p}_{i+1}). \tag{2}$$

The target-fixed frame is defined as $\{\Gamma_{obj}\}$, where the origin is at the center of the target object and the X_{obj}-, Y_{obj}- and Z_{obj} axes are parallel to the x-, y- and z-axes of the inertial frame, respectively. The projected vector of $\mathbf{r}_i$ onto the X_{obj}–Y_{obj} plane in the target-fixed frame is denoted as $\mathbf{d}_i$ and the scalars are defined as

$$\theta_i = \angle(\mathbf{e}_x, \mathbf{d}_i), \ \ \alpha_i = \angle(\mathbf{d}_i, \mathbf{r}_i), \ \ r_i := |\mathbf{r}_i|, \tag{3}$$

where $\mathbf{e}_x$ denotes the unit vector in the X_{obj}-direction of $\{\Gamma_{obj}\}$, and $\angle(\mathbf{x}, \mathbf{y})$ denotes the counterclockwise angle from vector $\mathbf{x}$ to vector $\mathbf{y}$. Then, $\mathbf{r}_i$ can be represented as

$$\mathbf{r}_i = [r_i \cos\theta_i \cos\alpha_i, \ r_i \sin\theta_i \cos\alpha_i, \ r_i \sin\alpha_i]^T. \tag{4}$$

Note that since $\mathbf{r}_{i+1} = \mathbf{r}_i - \mathbf{a}_i$, θ_{i+1} and ϵ_i, defined as

$$\epsilon_i = \begin{cases} \theta_{i+1} - \theta_i, & i = 1, 2, \cdots, n-1, \\ \theta_1 - \theta_n + 2\pi, & i = n, \end{cases} \tag{5}$$

can be calculated in a similar way based on (2). Let R denote the required distance between the target object and the agents.

Now we consider how to form a geometric pattern for the target-capturing task by the group of n agents. The detailed control objectives are stated as follows:

$(A1)$ n agents enclose the target object,*i.e.*, they are spaced out around the target object at intervals of assigned angles and maintain those angles.

$(A2)$ Each agent approaches the target object, maintaining a distance R.

$(A3)$ The angle α_i, which corresponds to the altitude of each agent, converges to the assigned angle Φ.

Note that for the sake of clarity and page limits, this paper only considers the equal convergence positions for all agents, *i.e.*, $R_1 = R_2 = \cdots = R_n = R$ and $\Phi_1 = \Phi_2 = \cdots = \Phi_n = \Phi$, whereas distinct positions for each agent can be assigned. In the following section, we will derive the control law that achieves objectives $(A1)$–$(A3)$.

3 Distributed Coordination Strategy

From the practical viewpoint, it is important to achieve the desired global behavior through relatively simple control laws using local information. We therefore propose a distributed coordination scheme for target-enclosing tasks, which can realize the required geometric formation mentioned in Section 2.

In order to develop such a control strategy, we first denote the assigned angular locations of θ_i ($i = 1, 2, \cdots, n$) by $\hat{\theta}_i$, which satisfies $0 \le \hat{\theta}_1 < \hat{\theta}_2 < \cdots < \hat{\theta}_n < 2\pi$. Thus, the control objectives ($A1$)–($A3$) presented in Section 2 can be formulated explicitly as follows:

($A1'$) $\theta_i(t) \to \hat{\theta}_i$[rad] as $t \to \infty$,

($A2'$) $r_i(t) \to R$ as $t \to \infty$,

($A3'$) $\alpha_i(t) \to \Phi$[rad] as $t \to \infty$ for $i = 1, 2, \cdots, n$.

Then, the proposed local control law for the ith agent P_i is described as

$$\dot{\theta}_i(t) = k_1 \delta\theta_i(t), \tag{6}$$

$$\dot{r}_i(t) = k_2(R - r_i(t)), \tag{7}$$

$$\dot{\alpha}_i(t) = k_3(\Phi - \alpha_i(t)), \tag{8}$$

where k_1, k_2, and k_3 (> 0) are the controller gains to be determined by the designer and

$$\begin{cases} \delta\theta_i(t) := \Psi_i \theta_{i+1}(t) - \theta_i(t), \ i = 1, 2, \cdots, n-1, \\ \delta\theta_n(t) := \Psi_n(\theta_1(t) + 2\pi) - \theta_n(t), \ i = n, \end{cases} \tag{9}$$

with $\Psi_i := \hat{\theta}_i / \hat{\theta}_{i+1}$ ($i = 1, 2, \cdots, n-1$) and $\Psi_n := \hat{\theta}_n / (\hat{\theta}_1 + 2\pi)$. Note that $0 \le \Psi_i < 1$ holds for any $i = 1, 2, \cdots, n$.

In order to analyze the overall multi-agent system, we rewrite (6) in the following vector form:

$$\dot{\theta}(t) = A\theta(t) + B, \tag{10}$$

where $\theta := [\theta_1, \theta_2, \cdots, \theta_n]^T \in \mathbb{R}^n$ and $A \in \mathbb{R}^{n \times n}$ and $B \in \mathbb{R}^n$ are

$$A := \begin{bmatrix} -k_1 & k_1\Psi_1 & 0 & \cdots & \cdots & 0 \\ 0 & -k_1 & k_1\Psi_2 & 0 & \cdots & 0 \\ \vdots & \ddots & \ddots & \ddots & \ddots & \vdots \\ 0 & \cdots & 0 & -k_1 & k_1\Psi_{n-2} & 0 \\ 0 & \cdots & \cdots & 0 & -k_1 & k_1\Psi_{n-1} \\ k_1\Psi_n & \cdots & \cdots & \cdots & 0 & -k_1 \end{bmatrix},$$

$$B := [0, \ 0, \ \cdots, \ 0, \ 2\pi k_1 \Psi_n]^T. \tag{11}$$

Next, key result (Geršgorin circle theorem), which is useful in stability analysis of our multi-agent systems will be presented [8].

Lemma 1 *Let M be a complex $n \times n$ with entries a_{ij}, where $i, j = 1, 2, \cdots, n$. For $i, j \in \{1, 2, \cdots, n\}$, define $\mathbf{R}_i = \sum_{j=1, i \ne j}^{n} |a_{ij}|$, where $|a_{ij}|$ denotes the complex norm of a_{ij}. Then, each eigenvalue of the matrix M is in at least one of the disks*

$$D_i(M) = \{z \in \mathbf{C} : |z - a_{ii}| \le \mathbf{R}_i, i = 1, 2, \cdots, n\} \tag{12}$$

in the complex plane. Equivalently, the n eigenvalues of M are contained in the region in the complex plane determined by

$$D(M) = \bigcup_{i=1}^{n} D_i(M). \tag{13}$$

Note that $a_{ii} = -k_1$ and $0 \le \mathbf{R}_i (= |k_1 \Psi_i|) < k_1$ of the matrix A in (11), since $0 \le \Psi_i < 1$ and $k_1 > 0$ for $i = 1, 2, \cdots, n$. Hence, from Lemma 3.1, it can be easily verified that the n eigenvalues λ_i ($i = 1, 2, \cdots, n$) of the matrix A are in the set $\Lambda := \{\lambda \in \mathbf{C} : \mathrm{Re}(\lambda) < 0\}$, where $\mathrm{Re}(\lambda)$ denotes the real part of $\lambda \in \mathbf{C}$. Then, the main result of the paper is stated as follows:

Theorem 2 *Consider the system of n agents. It is assumed that all agents are initially arranged in 3D space as shown in Figure 1. Then, control laws (6)–(8) achieve ($A1'$)–($A3'$) simultaneously.*

Proof. Since it is obvious that (7) implies ($A2'$) and (8) implies ($A3'$), we will prove that ($A1'$) is achieved. Define $e_i := \theta_i - \hat{\theta}_i$. Note that $A\hat{\theta} + B = 0$, where $\hat{\theta} := [\hat{\theta}_1, \hat{\theta}_2, \cdots, \hat{\theta}_n]^T \in \mathbb{R}^n$. Then, it follows from (10) that $\dot{e}(t) = Ae(t)$, where $e := [e_1, e_2, \cdots, e_n]^T \in \mathbb{R}^n$ and A is a stable matrix, as shown in Lemma 3.1. Therefore, it holds that $e(t) \to 0$ as $t \to \infty$. □

The above theorem implies that the control laws given in (6)–(8) guarantee that all agents assemble into the assigned formation around the freely moving target object in 3D space. The control scheme has additional distinctive features, in that each agent individually obtains the required information using the sensor systems implemented on its body, which means that no communication mechanism between agents is introduced. In addition, it is a memoryless controller in the sense that agent P_i ($i = 1, 2, \cdots, n$) determines its next behavior based only on the current information on agent P_{i+1}, independently of the past behavior of P_{i+1}. Thus, it is an easily implementable method from the engineering viewpoint. Moreover, it is a practical method because it is robust against any finite number of transient measurement errors (*e.g.*, cases in which agent P_{i+1} is invisible from agent P_i for a period of time). These properties will be verified through simulation studies in the following section (see Section 4.2).

It may be in order to describe $\mathbf{u}_i$ explicitly. From (1), (2), and (4), it is straightforward to obtain

$$\mathbf{u}_i = \dot{\mathbf{r}}_i + \dot{\mathbf{p}}_o \tag{14}$$

subject to (6)–(8). Note that it is inevitable to exploit $\dot{\mathbf{p}}_o$ in order to achieve target capturing without any errors irrespective of the control strategies. When each agent knows the target velocity in the steady state, $(A1')$–$(A3')$ will be satisfied. We will evaluate the performance in the case where $\dot{\mathbf{p}}_o$ is not available at all in Section 4.

On the other hand, the full actuation agent is considered in this paper, but there are times when full actuation may be infeasible because of the actuator limitation. As one of the possible methods to overcome such a problem, we can set constraints on $\dot{\theta}_i$, $\dot{r}_i$, and $\dot{\alpha}_i$ $(i = 1, 2, \cdots, n)$ in (6)–(8) as

$$|\dot{\theta}_i(t)| \leq \theta_{i,\max},\ |\dot{r}_i(t)| \leq r_{i,\max},\ |\dot{\alpha}_i(t)| \leq \alpha_{i,\max}, \tag{15}$$

for $\forall t \geq 0$, where $\theta_{i,\max}$, $r_{i,\max}$, and $\alpha_{i,\max}$ are given by the designer. In Sections 4.1 and 4.2, we will demonstrate that the control objectives $(A1')$–$(A3')$ can be achieved without problem even when the control laws (6)–(8) subject to (15) are applied.

Next, we consider the collision avoidance problem. The proposed distributed coordination control laws (6)–(8) cannot guarantee that no collision occurs; *e.g.*, if $\Psi_i(t) \approx 0$, which probably results in $\dot{\theta}_i(t) < 0$, agent P_i may collide with agent P_{i-1}, which satisfies $\dot{\theta}_{i-1}(t) > 0$, $\epsilon_{i-1}(t) > 0$, $r_{i-1}(t) = r_i(t)$, and $\alpha_{i-1}(t) = \alpha_i(t)$. In order to decrease the possibility of collisions, we consider the following: Consider that n agents are dispersed in a counterclockwise star formation ([6, 7, 9]) at the initial time instant (see Figure 1, where $d_i > 0$, $0 < \epsilon_i < 2\pi$ for $i = 1, 2, \cdots, n$, and $\sum_{i=1}^{n} \epsilon_i = 2\pi$). Then, we redefine the assigned angular locations $\bar{\theta}_i$ of θ_i and Ψ_i in (9) as

$$\begin{aligned} &\bar{\theta}_i := \hat{\theta}_i + 2\ell\pi,\ i = 1, 2, \cdots, n, \\ &\Psi_i := \bar{\theta}_i / \bar{\theta}_{i+1},\ i = 1, 2, \cdots, n-1, \\ &\Psi_n := \bar{\theta}_n / (\bar{\theta}_1 + 2\pi), \end{aligned} \tag{16}$$

where ℓ denotes the positive integer. Note that $0 < \Psi_i < 1$ holds for any $i = 1, 2, \cdots, n$, and thus the convergence property given in Theorem 3.2 is also preserved. However, for $\ell \gg 1$, one can obtain $\Psi_i \approx 1$. Therefore, (16) has all agents circulating in a counterclockwise direction, finally converging to their assigned locations $\hat{\theta}_i$ for $i = 1, 2, \cdots, n$. Note that if $\Psi_i = 1$, no collision occurs, as shown in Kim and Sugie [6, 7]. Thus we can see that the above simple technique (16) would be useful for collision avoidance. Its effectiveness will be demonstrated through numerical examples in Section 4.3. Note that a clockwise formation can be treated in a similar way.

Parameters of the initial location

P_i	1	2	3	4	5	6	7	8	9	10
θ_i	0.95	1.63	1.84	2.10	2.36	2.62	2.88	3.14	3.40	3.67
r_i	22	30	25	13	20	15	29	26	21	16
α_i	1.10	1.36	1.23	1.30	1.05	1.25	1.20	0.70	1.40	0.90

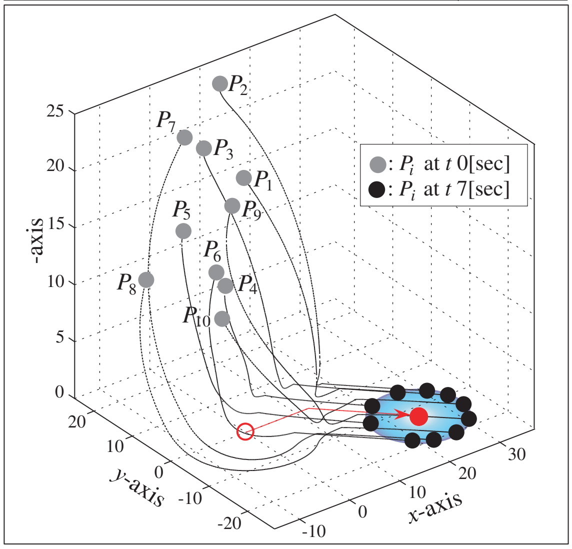

Figure 2: Simulation result of Case 1: Position trajectories of P_i $(i = 1, 2, \cdots, 10)$.

4 Simulation examples

In this section, the performance of the coordination strategy proposed in Section 3 is evaluated in the case where $\dot{\mathbf{p}}_o$ is not available at all,*i.e.*, $\dot{\mathbf{p}}_o(t) = \mathbf{0}$ in (14).

4.1 Case 1

To illustrate the dynamic performance of the proposed distributed coordination scheme, a simulation is carried out in which $n = 10$ agents are initially randomly dispersed in 3D space before finally achieving the required formation stated in Sections 2–3. Specifically, the assigned locations $\hat{\theta}_i$, R, and Φ for P_i $(i = 1, 2, \cdots, 10)$ are determined as follows: $R = 8$, $\Phi = 0$, $\hat{\theta}_1 = 0.3$, $\hat{\theta}_2 = 0.75$, $\hat{\theta}_3 = 1.35$, $\hat{\theta}_4 = 2.1$, $\hat{\theta}_5 = 2.8$, $\hat{\theta}_6 = 3.93$, $\hat{\theta}_7 = 4.36$, $\hat{\theta}_8 = 4.90$, $\hat{\theta}_9 = 5.5$, and $\hat{\theta}_{10} = 6.1$. The initial locations of agents are chosen as shown in Figure 2. The controller gains k_1, k_2, and k_3 in (6)–(8) are chosen as $k_1 = k_2 = k_3 = 5$. The sampling time is $t_s = 0.01$[s] and the simulation is performed for $t = 7$[s]. The path of the target object

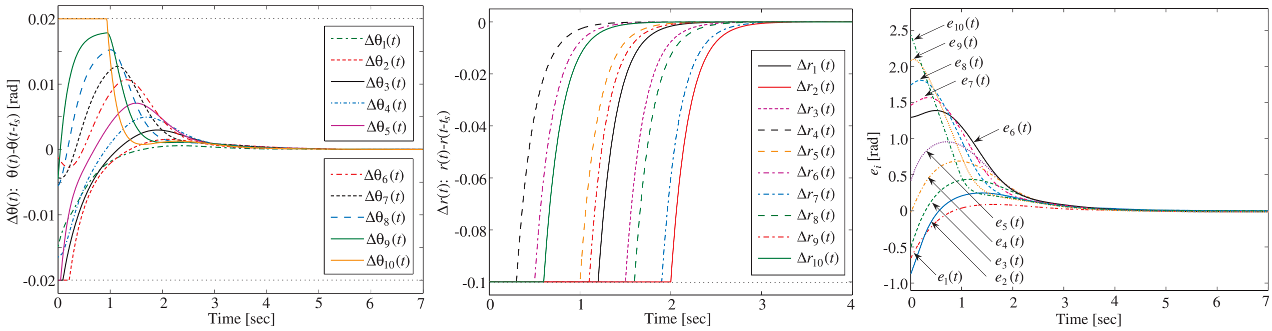

(a) Time plots of $\Delta\theta_i(t)$[rad] (b) Time plots of $\Delta r_i(t)$ $(i = 1, 2, \cdots, 10)$ (c) Time plots of $e_i(t)$[rad]

Figure 3: Simulation results of Case 1: Time plots of $\Delta\theta_i(t)$, $\Delta r_i(t)$, and $e_i(t)$ $i = 1, 2, \cdots, 10$.

is set as follows: $\mathbf{p}_o(t) = [5t, 0, 0]^T$ for $t \in [0, 2.5]$; $\mathbf{p}_o(t) = [5t, -5(t-2.5), 0]^T$ for $t \in (2.5, 5]$; $\mathbf{p}_o(t) = [25, -12.5, 0]^T$ for $t \in (5, 7]$. Note that each agent does not know $\dot{\mathbf{p}}_o(t)$ [*i.e.*, $\dot{\mathbf{p}}_o(t) = \mathbf{0}$ in (14)]. It is supposed that $\Delta\theta_i(t) := \theta_i(t) - \theta_i(t-t_s)$, $\Delta r_i(t) := r_i(t) - r_i(t-t_s)$, and $\Delta\alpha_i(t) := \alpha_i(t) - \alpha_i(t-t_s)$ $(i = 1, 2, \cdots, 10)$ for $t \in (0, 7]$ are constrained as

$$\Delta\theta_i(t) = \begin{cases} 0.02, & \text{if } \Delta\theta_i(t) > 0.02 \\ \Delta\theta_i(t), & \text{if } |\Delta\theta_i(t)| \le 0.02 \\ -0.02, & \text{if } \Delta\theta_i(t) < -0.02 \end{cases} \tag{17}$$

$$\Delta r_i(t) = \begin{cases} 0.1, & \text{if } \Delta r_i(t) > 0.1 \\ \Delta r_i(t), & \text{if } |\Delta r_i(t)| \le 0.1 \\ -0.1, & \text{if } \Delta r_i(t) < -0.1 \end{cases} \tag{18}$$

$$\Delta\alpha_i(t) = \begin{cases} 0.01, & \text{if } \Delta\alpha_i(t) > 0.01 \\ \Delta\alpha_i(t), & \text{if } |\Delta\alpha_i(t)| \le 0.01 \\ -0.01, & \text{if } \Delta\alpha_i(t) < -0.01 \end{cases} \tag{19}$$

The simulation results are shown in Figures 2 and 3. First, Figure 2 illustrates the resulting position trajectories of a group of ten agents during the simulation; the agents assemble into the assigned configuration and track the freely moving target object simultaneously. The time plots of $\Delta\theta_i(t)$ and $\Delta r_i(t)$ are shown in Figures 3(a) and 3(b), which verify that constraints (17)–(18) are satisfied. Also, $\Delta\theta_i(t)$ satisfies (19) and its time plot is similar to Figure 3(b). The changes of $e_i := \hat{\theta}_i - \theta_i$ $(i = 1, 2, \cdots, 10)$ with respect to time are plotted in Figure 3(c), where all e_i values finally converge to zero. The results show that all agents converge to the assigned formation around the target object and maintain their coordinates. The above simulation results clearly demonstrate that control goals $(A1')$–$(A3')$ mentioned in Section 3 are achieved by the developed simple distributed control laws, (6), (7), and (8), subject to constraints (17), (18), and (19).

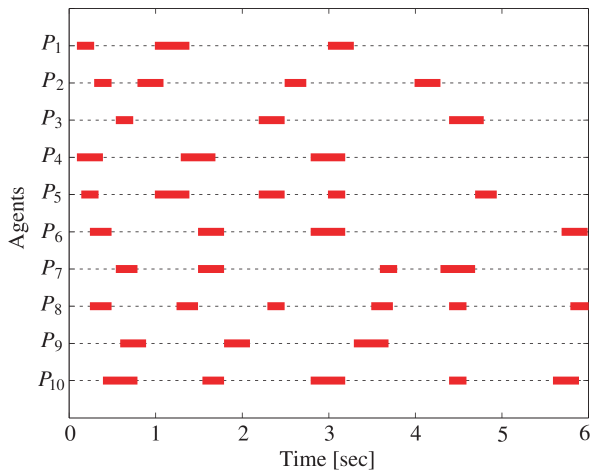

Figure 4: Interval of invisibility for P_i $(i = 1, 2, \cdots, 10)$.

4.2 Case 2

To consider a more realistic scenario, it is assumed that agent P_{i+1} is invisible from agent P_i for a period of time, $t \in [t_{i_1}, t_{i_2}]$, shown in Figure 4. This means that the ith agent P_i might be unable to take the measurement of $\mathbf{a}_i$, and thus θ_{i+1} is unavailable in control law (6). In this case, we can set $\delta\theta_i$ as $\delta\theta_i(t) = \delta\theta_i(t_{i_1} - t_s)$, where $t \in [t_{i_1}, t_{i_2}]$. Simulations are performed in the case of $n = 10$ agents, with the same initial parameters given in Section 4.1. Similar to the Case 1, it is assumed that each agent does not know $\dot{\mathbf{p}}_o(t)$ and that $\Delta\theta_i(t)$, $\Delta r_i(t)$, and $\Delta\alpha_i(t)$ are constrained as (17)–(19). The assigned final locations for P_i $(i = 1, 2, \cdots, 10)$ are given in Figure 5. The path for the target object is set as follows: $\mathbf{p}_o(t) = [5t, -5t, 0]^T$ for $t \in [0, 2.5]$; $\mathbf{p}_o(t) = [5t, -12.5, 0]^T$ for $t \in (2.5, 5]$; $\mathbf{p}_o(t) = [25, -12.5, 0]^T$ for $t \in (5, 6]$.

The transient motions of agents for $t = 6$[s] are shown in Figure 5. In addition, the time plots of $e_i(t)$ are given in Figure 6, which shows that the proposed

Parameters of the assigned location

P_i	1	2	3	4	5	6	7	8	9	10
θ_i	0	0.541	1.031	$\pi/2$	$3\pi/4$	π	$5\pi/4$	$3\pi/2$	5.253	5.743
r_i	8	5.83	5.83	8	5.66	8	5.66	8	5.83	5.83
α_i	0	0	0	0	0	0	0	0	0	0

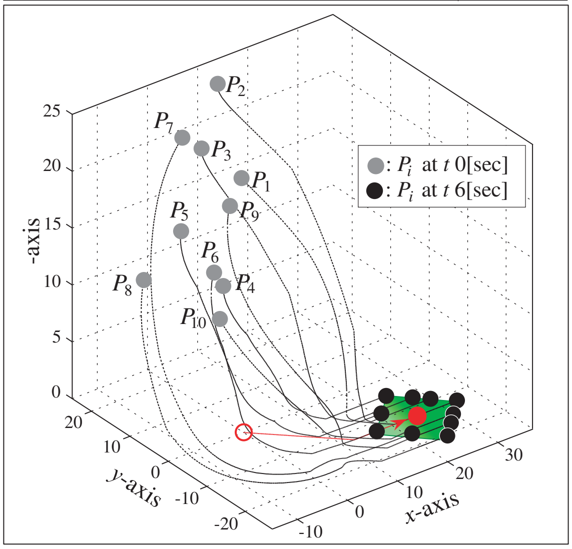

Figure 5: Simulation result of Case 2: Position trajectories of P_i $(i = 1, 2, \cdots, 10)$.

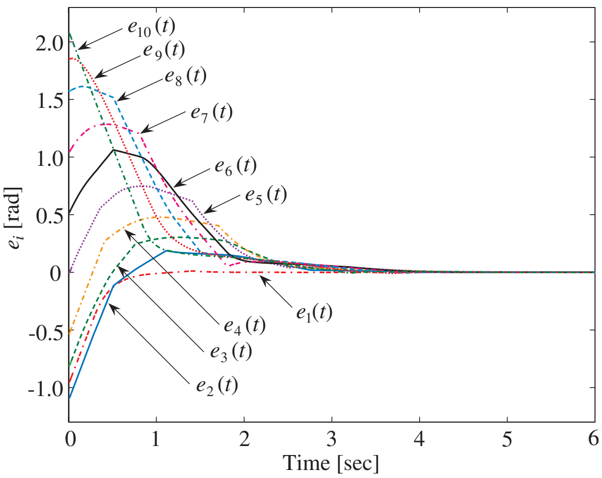

Figure 6: Time plots of $e_i(t)$[rad] $(i = 1, 2, \cdots, 10)$.

Parameters of the assigned location

P_i	1	2	3	4	5	6	7	8	9	10
θ_i	0.1	0.3	0.5	0.7	0.9	1.1	1.3	1.5	1.7	1.9
r_i	8	8	8	8	8	8	8	8	8	8
α_i	0	0	0	0	0	0	0	0	0	0

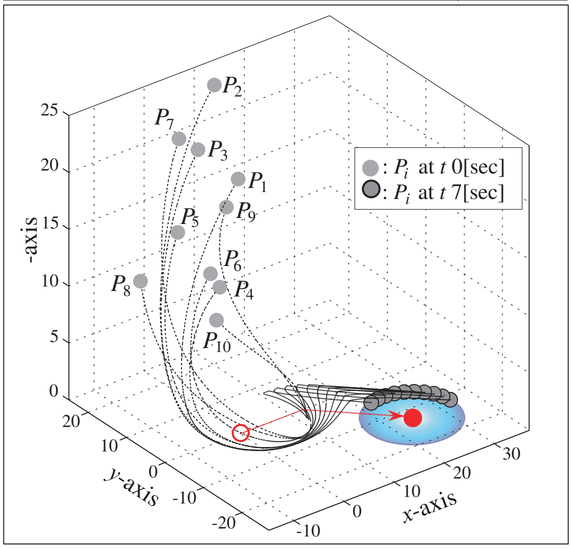

Figure 7: Simulation result of Case 3: Position trajectories of P_i $(i = 1, 2, \cdots, 10)$.

scheme is sufficiently robust against any finite number of transient measurement errors. The behaviors of all agents demonstrate the achievement of the convergence scenario outlined in the previous sections and verify the distinctive feature of the robust memoryless control scheme.

4.3 Case 3

In Section 3, we proposed a method to lessen the possibility of a collision between agents. Here we will demonstrate its effectiveness. The initial locations of agents are identical to those used in Section 4.2. Their assigned final positions are given in Figure 7. The controller gain k_1 in (6) is set as $k_1 = 15$. Other design parameters and the target's path are set identically to those of Section 4.2. Constraints such as (17)–(19) are not considered. Note that ten agents are initially dispersed in a counterclockwise star formation ([9, 6, 7]),*i.e.*, $\theta_i(0) < \theta_{i+1}(0)$ holds. If we perform the simulation based on (6)–(8) under the above setting, a counterclockwise star formation is not preserved. This means that a case such as $\theta_i(t) > \theta_{i+1}(t)$ happens at some time instant. Note that the above situation could lead to a collision between agents.

In order to avoid a collision, we introduce the technique given in (16). The assigned angular locations are set as $\bar{\theta}_i := \hat{\theta}_i + 2\pi$ $(i = 1, 2, \cdots, 10)$, where the values of $\hat{\theta}_i$ are given in Figure 7. Then, $\Psi_i :=$

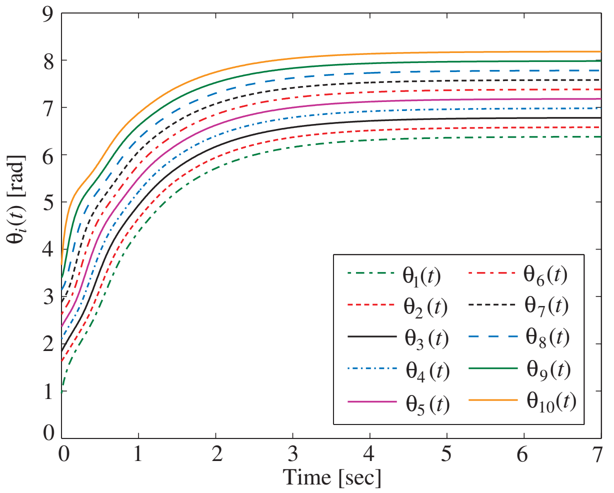

Figure 8: Time plots of $\theta_i(t)$[rad] $(i = 1, 2, \cdots, 10)$.

$\bar{\theta}_i/\bar{\theta}_{i+1}$ $(i = 1, 2, \cdots, 9)$ and $\Psi_{10} := \bar{\theta}_{10}/(\bar{\theta}_1 + 2\pi)$ are used in control law (6) with (9). The simulation results are illustrated in Figures 7 and 8. They show that all agent circulate in a counterclockwise direction and then converge to the assigned locations. Further, Figure 8 demonstrates that a counterclockwise star formation is preserved and no collisions occur between agents. From the above results, we can see that the proposed simple collision avoidance technique (16) in Section 3 is a feasible one in our coordination scheme.

5 Conclusion

In this paper, we have proposed a simple distributed coordination strategy for a target-enclosing operation by particle swarms. In this scheme, multiple agents are controlled in a very simple distributed manner so as to converge to the formation assigned by the designer while tracking a target object moving in 3D space. To that purpose, each agent individually decides its behavior using only locally available information,*i.e.*, distances and angles with respect to other agents and to the target objective. Therefore, instead of the use a global information and/or communication mechanism, only local sensor systems need to be adopted to generate the desired global group behavior. This means that this scheme can reduce the information requirements as compared with conventional methods. From these viewpoints, the proposed method is easily implemented. Furthermore, it appears to be a practical method for the following reasons: (i) it is robust against any finite number of transient measurement errors and (ii) it can achieve the control objectives even when constraints on the control input exists. One of the schemes to decrease the possibility of collisions between agents has also been proposed. Numerical examples have illustrated the efficacy of the proposed method.

Future research will be devoted to extending the proposed methodology to handle agents with dynamics and motion constraints. Also, in order to improve the implementability of the proposed scheme, a method of estimating the velocity of the target object should be developed. Further, the scheme should be tested experimentally to investigate its performance in a realistic environment.

Acknowledgements: This research was supported by Basic Science Research Program through the National Research Foundation of Korea (NRF) funded by the Ministry of Education, Science and Technology (No. 2012-012295).

References:

[1] A. Sinha and D. Ghose, Generalization of the cyclic pursuit problem, *Proceedings of American Control Conference*, 2005, pp. 4997–5002.

[2] J. A. Marshall, M. E. Broucke and B. A. Francis, Formations of vehicles in cyclic pursuit, *IEEE Transactions on Automatic Control*, 49(11), 2004, pp. 1963–1974.

[3] J. A. Marshall, M. E. Broucke and B. A. Francis, Pursuit formations of unicycles, *Automatica*, 42, 2006, pp. 3–12.

[4] K. Kobayashi, K. Otsubo and S. Hosoe, Design of decentralized capturing behavior by multiple robots, *IEEE Workshop on Distributed Intelligent Systems: Collective Intelligence and its applications*, 2006, pp. 463–468.

[5] R. Sepulchre, D. A. Paley and N. E. Leonard, Group coordination and cooperative control of steered particles in the plane, *Group Coordination and Cooperative Control*, Springer-Verlag: Lecture Notes in Control and Information Sciences, 2006, pp. 217–232.

[6] T.-H. Kim and T. Sugie, Cooperative control for target capturing based on a cyclic pursuit strategy, *The 35th SICE Symposium on Control Theory*, 2006, pp. 361–366.

[7] T.-H. Kim and T. Sugie, Cooperative control for target-capturing task based on a cyclic pursuit strategy, *Automatica*, 43, 2007, pp. 1426–1431.

[8] R. A. Brualdi and S. Mellendorf, Regions in the complex plane containing the eigenvalues of a matrix, *The American Mathematical Monthly*, 101(10), 1994, pp. 975–985.

[9] Z. Lin, M. E. Broucke and B. A. Francis, Local control strategies for groups of mobile autonomous agents, *IEEE Transactions on Automatic Control*, 49, 2004, pp. 622–629.